Supporting Information

Predicting the breakthrough performance of "gating" adsorbents using osmotic framework adsorbed solution theory

*Francisco J. Sotomayor, Christian M. Lastoskie**

Department of Civil and Environmental Engineering, University of Michigan, Ann Arbor, Michigan 48109-2125

Table of Contents

Section S1. Material Characterization. Characterization of the materials was done by collecting X-ray powdered diffraction (XRD) patterns on a Rigaku MiniFlex600 and infrared (IR) spectra on a PerkinElmer Spectrum BX FT-IR spectrometer. XRD and IR patterns for pre-ELM-11 are shown in Figures S1 and S2 respectively.

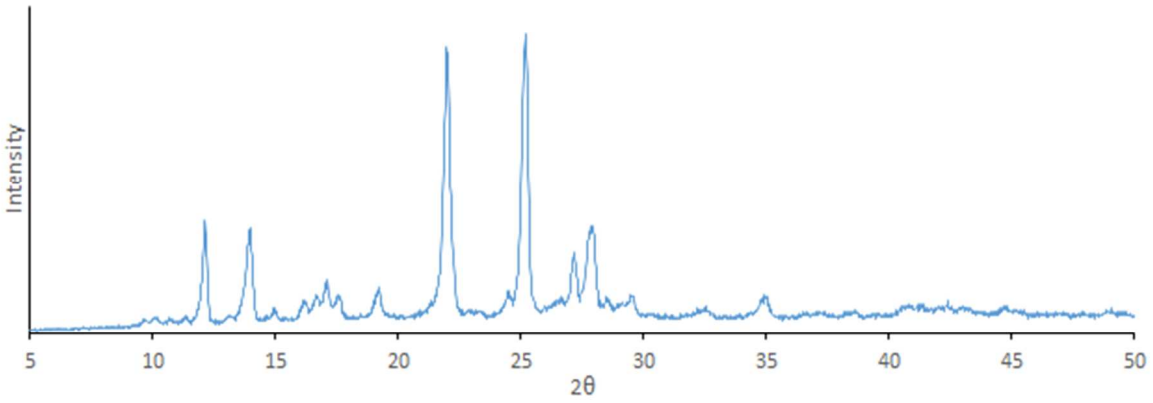

Figure S1. XRD pattern for pre-ELM-11.

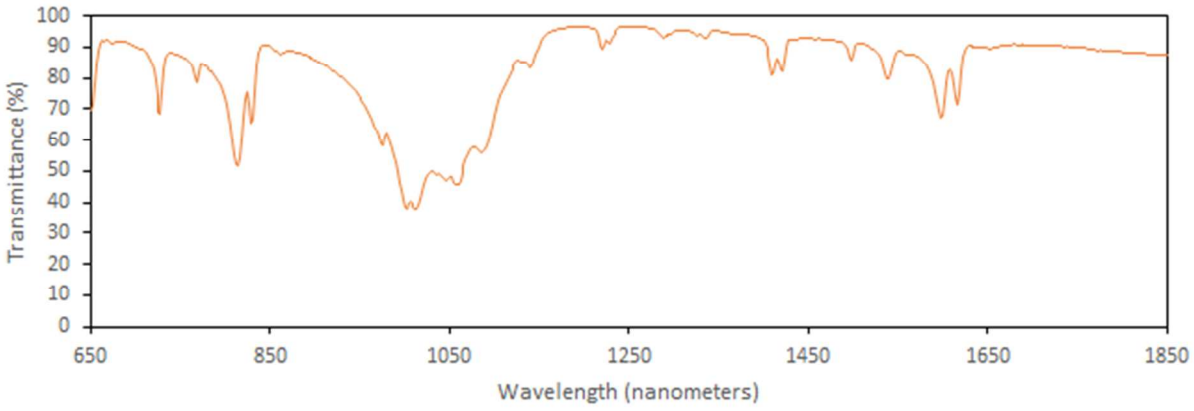

Figure S2. IR spectrum for pre-ELM-11.

Section S2. Breakthrough Experimental Setup. A schematic of the gas flow apparatus built in-house is shown in Figure S3. Flow rates of CO_2, CH_4, N_2, and He were controlled using needle valves and the overall flow speed was tracked using a rotameter. Gas pressure within the adsorbent bed was held at slightly above atmospheric pressure (~108 kPa) to prevent infiltration of room air into the experimental system. The gas flowrate through the column was between 0.5 and 2.0 ml/min. Ions of molecular weight 44 and 28 were used to measure the CO_2 breakthrough and release curves. Ions of molecular weight 4, 13, 14, and 15 provided supplemental information on the gas species He, CH_4, and N_2. Ions of molecular weight 18 were used to identify if any water vapor from the temperature bath or room air had infiltrated the column.

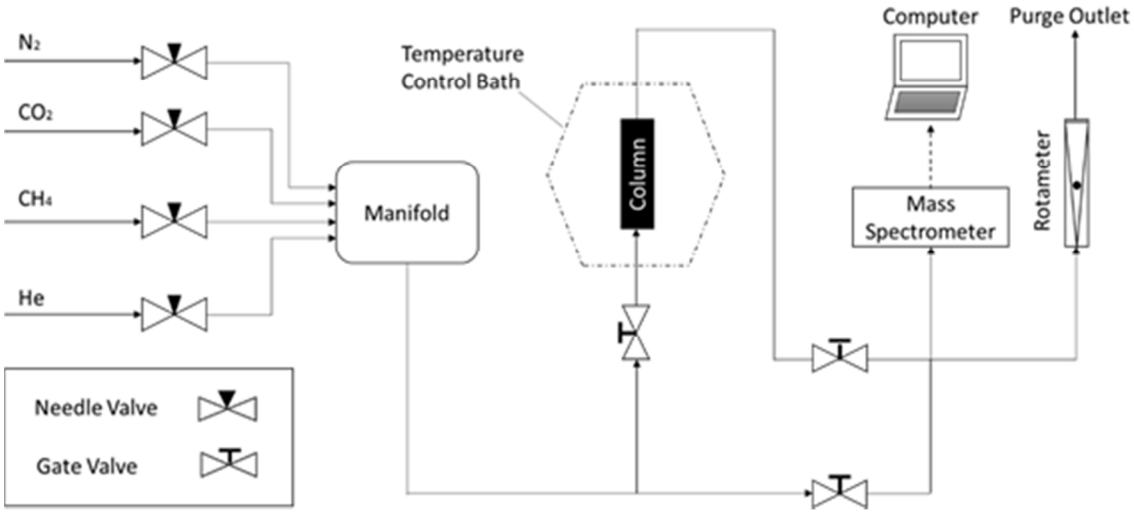

Figure S3. Schematic of laboratory apparatus for breakthrough experiments.

Section S3. OFAST Model Development. A summary of the different OFAST model types is shown in Table S1. Model 1 relies on the experimental CO_2 isotherms to estimate P_{gate}, N_{max}, and K as a function of temperature. These estimates were obtained as follows. First, Langmuir fits were applied to the experimental CO_2 isotherms at 273, 308, 318, and 338 K, as shown in Figure S4. Once Langmuir fits for a range of temperatures were obtained, N_{max} and K as a function of temperature were determined graphically, as shown in Figure S5.

Table S1. Summary of OFAST Model Types

<table>
<tr><th>OFAST Model</th><th>Gas Mixture Assumption</th><th>$P_{gate}(T)$*</th><th>$N_{max}(T)$</th><th>K(T)</th></tr>
<tr><td>Model 1</td><td>pure CO_2</td><td rowspan="2">CO_2 isotherm</td><td colspan="2">CO_2 isotherm Langmuir fit</td></tr>
<tr><td>Model 2</td><td rowspan="2">CO_2/He
CO_2/N_2
CO_2/CH_4</td><td colspan="2" rowspan="2">mixed gas modeling IAST</td></tr>
<tr><td>Model 3</td><td>breakthrough curves</td></tr>
</table>

*For Model 2, $\Delta F^{host}(T)$ was assumed to match the values obtained for Model 1. $P_{gate}(T)$ was then back-calculated using IAST estimates of $N_{max}(T)$ and $K(T)$.

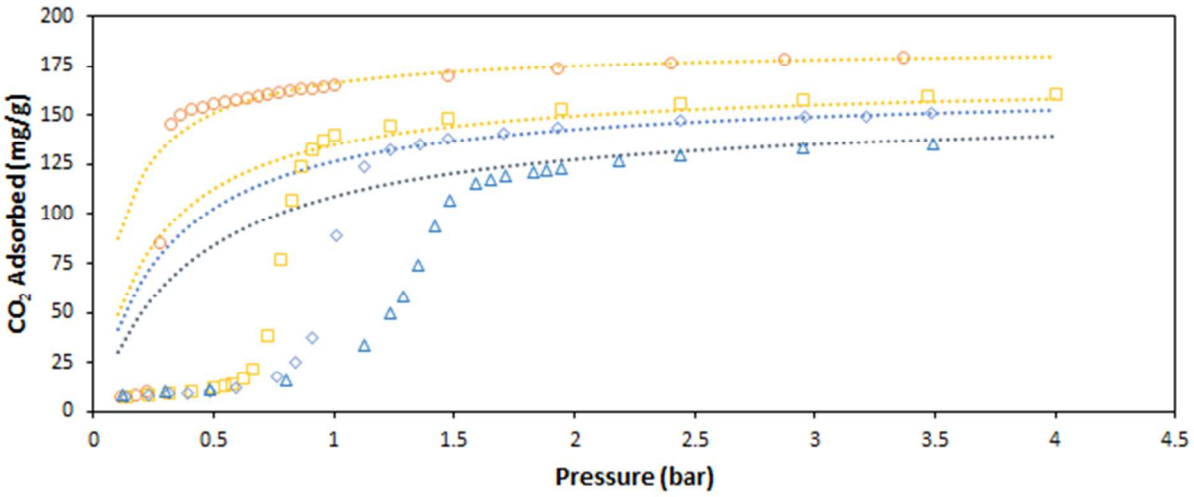

Figure S4. Langmuir fits of experimental CO_2 isotherms at 273 (orange circles), 308 (yellow squares), 318 (light blue diamonds), and 338 K (dark blue triangles). Desorption branches only. Sorption branches are removed for clarity. Langmuir fits of the experimental data are shown as dashed lines.

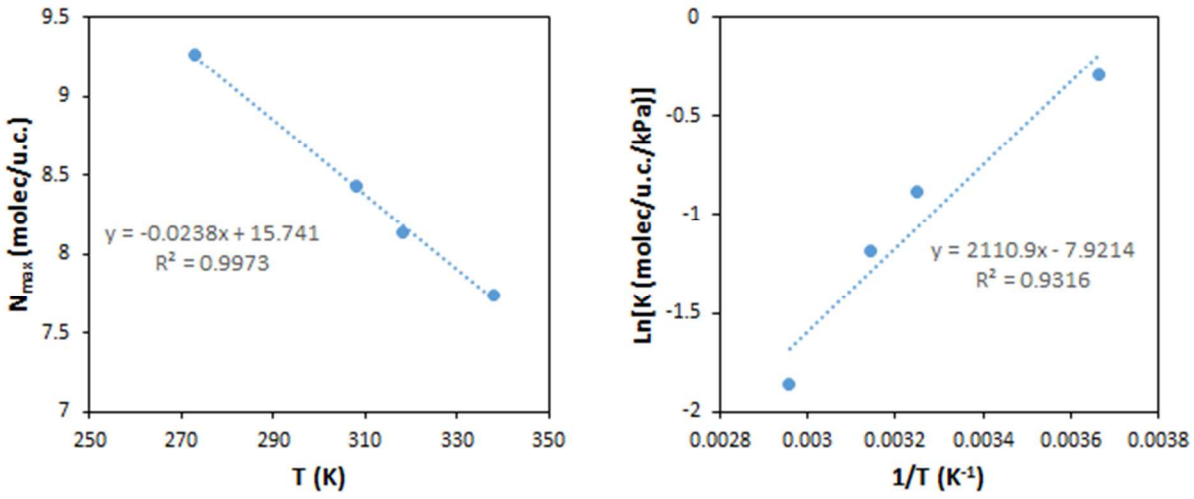

Figure S5. Variation of Langmuir parameters with temperature for CO_2 adsorption. Left: N_{max} (molecules/unit cell) vs T (K); right: ln[K (molecules/unit cell/kPa)] vs $1/T$ (K^{-1}).

After determining N_{max} and K as a function of temperature, it is necessary to estimate the gate pressure for each of the experimental isotherms in order to develop an estimate for $\Delta F^{host}(T)$. At low temperature there is little ambiguity in the gate pressure, as the experimental isotherm is nearly a vertical line at the gating transition. However, at high temperature the gate pressure is not distinct, with significant smoothing of the gate transition. In order to provide a non-arbitrary, repeatable measurement of the gate pressure even at high temperature, the range for the gate pressure is defined herein as the pressures between the minimum and maximum of the second derivative of the experimental isotherm. For a single-point gate pressure measurement, the gate pressure is defined herein as the average of the pressures at the minimum and maximum of the second derivative. For the example shown in Figure S6, the gate pressure would range from 790 to 973 mmHg, and the single-point measurement of the gate pressure would be 882 mmHg.

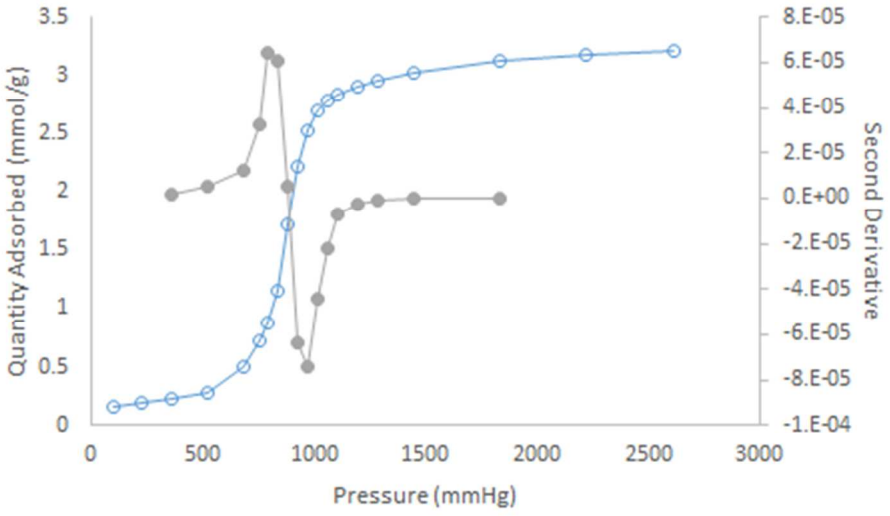

Figure S6. Determination of the gate pressure from the desorption branch of the CO_2 isotherm measured at 328 K. The experimental isotherm is shown as the blue open circles and the second derivative of the isotherm is shown as the grey,solid circles.

Once estimates of the gate pressure are determined, ΔF^{host} can be estimated for each measured temperature and an equation for $\Delta F^{host}(T)$ can be generated. A logistic fit of the ΔF^{host} values best represented the data for ELM-11 for temperatures ranging from 250 to 350 K.

For the desorption branch:

$$\Delta F^{host}(T)\left[\frac{J}{mol}\right] = \frac{32173.9}{1+8.989x10^{6}*EXP(-0.06357*T)} \quad (S1)$$

For the adsorption branch:

$$\Delta F^{host}(T)\left[\frac{J}{mol}\right] = \frac{38445.4}{1+5.535x10^{6}*EXP(-0.06272*T)} \quad (S2)$$

Measured P_{gate} values and the OFAST model fit for both gate opening (adsorption) and gate closing (desorption) are compared in Figure S7. Figure S8 compares examples of the overall fit of Model 1 with the desorption branches of the experimental CO_2 adsorption isotherms. As can be seen in Figures S7 and S8, Model 1 reasonably replicates both the expected CO_2 capacity and the gate pressure for static ELM-11 isotherms measured over a range of temperatures.

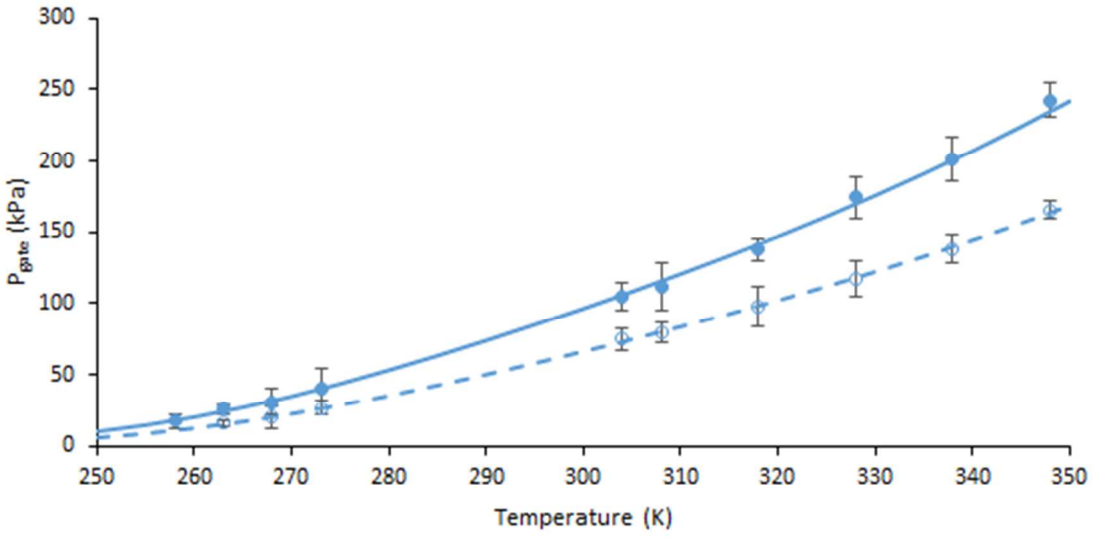

Figure S7. Comparison of experimental gate pressure (points) with Model 1 (lines). Dashed line and open symbols represent gate closing (desorption branch). Solid line and closed symbols represent gate opening (adsorption). Error bars represent the width of the gate as measured by the distance between the maximum and minimum in the second derivative of the sorption curve.

For Model 2, it is assumed that free energy difference (ΔF^{host}) between the collapsed and open framework structure estimated for Model 1 has not changed. However, instead of solely using the Langmuir fit of the experimental CO_2 isotherms to determine N_{max} and K, mixed gas adsorption is assumed and ideal gas adsorbed solution theory (IAST) is used to determine mixture co-adsorption on the expanded ELM-11 structure. To obtain IAST estimates for the gas mixtures, both the experimental CO_2 isotherms in Figure S4 and additional pure component isotherms for He, N_2, and CH_4 obtained from GCMC simulations are used. First, Langmuir parameters for the He, N_2, and CH_4 isotherms are fitted to GCMC simulation results as shown respectively in Figures S9-S11.

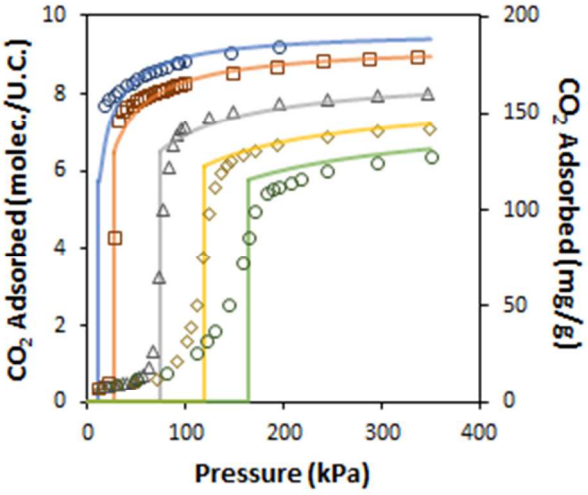

Figure S8. Comparison of Model 1 predictions (lines) with desorption branches of the experimental CO_2 isotherms (points) at 258 (blue circles), 273 (red squares), 304 (grey triangles), 328 (yellow diamonds) and 348 K (green circles). Adsorption branches were removed for clarity. Vertical axis scale values for total CO_2 adsorbed are presented in both molecules per unit cell (left) and mg-CO_2 per g-ELM-11 (right).

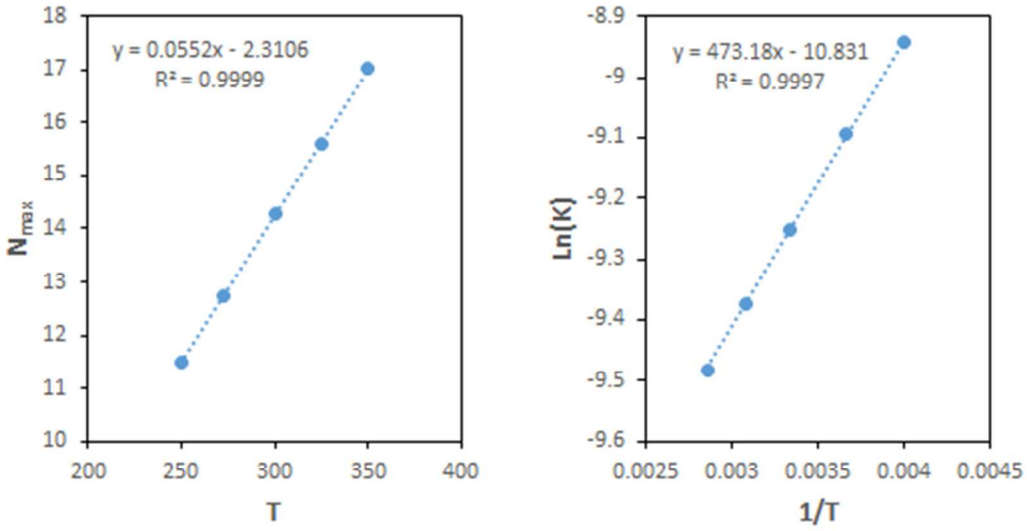

Figure S9. Variation of Langmuir parameters with temperature for He adsorption. Left: N_{max} (molecules/unit cell) vs T (K); right: ln[K (molecules/unit cell/kPa)] vs $1/T$ (K^{-1}).

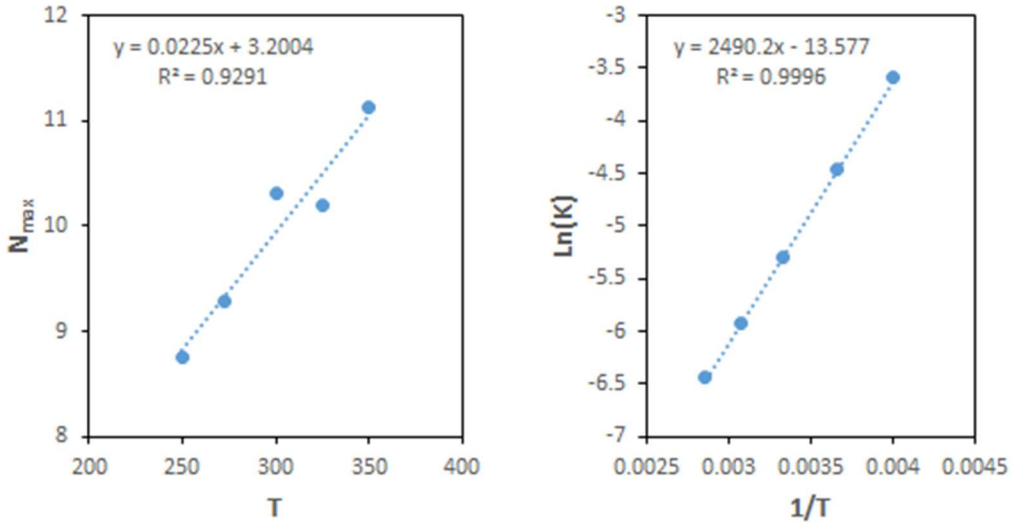

Figure S10. Variation of Langmuir parameters with temperature for N_2 adsorption. Left: N_{max} (molecules/unit cell) vs T (K); right: ln[K (molecules/unit cell/kPa)] vs $1/T$ (K^{-1}).

Once the Langmuir parameters for all of the single component isotherms are known, the total amount of a gas mixture adsorbed at a particular temperature, pressure, and mixture composition is found numerically by solving the IAST systems of equations as described by Coudert[1]. In the current work, the numerical solution was found using a custom code in MATLAB[2]. A sample code that estimates P_{gate} using OFAST and IAST is shown in Section S5.

For Model 3, it is assumed that the mixture co-adsorption isotherm parameters (N_{max} and K) obtained for Model 2 are the same. But instead of using single component CO_2 isotherms to estimate P_{gate}, estimates of P_{gate} are obtained directly from the breakthrough experiments for the different gas mixtures. As in the case of the gating transition, the step height is not a distinct point, with significant smoothing of the step occurring at high temperatures. To provide non-arbitrary, repeatable measurements of the step height observed in breakthrough experiments, the single point measurement of the step height is defined herein as the median value of the

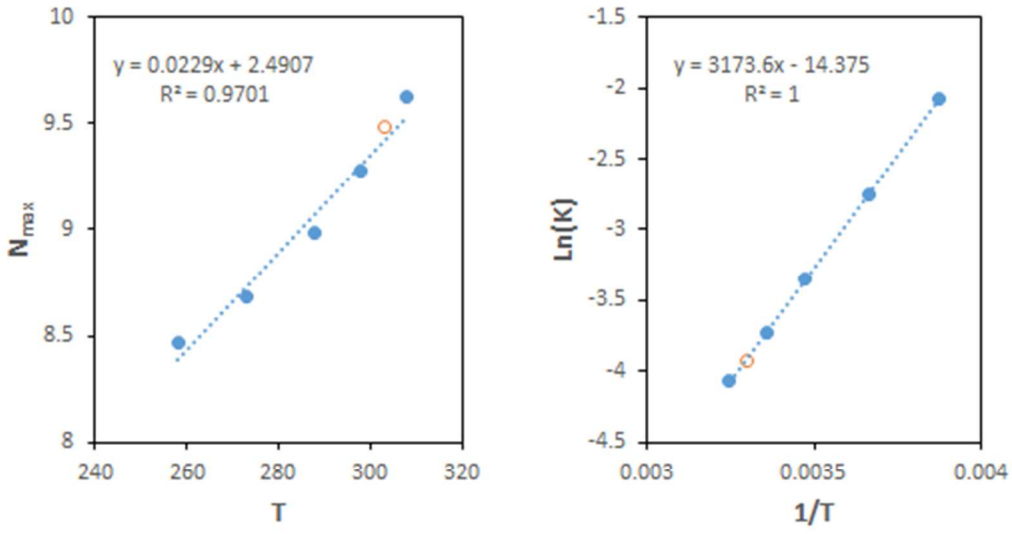

Figure S11. Variation of Langmuir parameters with temperature for CH_4 adsorption. Left: N_{max} (molecules/unit cell) vs T (K); right: ln[K (molecules/unit cell/kPa)] vs $1/T$ (K^{-1}). Closed symbols represent points used for trend line fit; open symbol represents a simulated value not included in the trend line fit.

experimental points between the two peaks in the first derivative of the breakthrough curve. For the example shown in Figure S12, the time stamps included in the step anomaly would range from 0.731 to 4.072 minutes, and the single point measurement of the step level would be a n effluent CO_2 fraction of 0.632.

Once estimates of the step levels are determined, ΔF^{host} is estimated for each measured temperature and mixture composition and an equation for $\Delta F^{host}(T)$ is generated from each breakthrough measurement. A linear fit was used for each gas mixture to determine the temperature dependence of ΔF^{host} for temperatures ranging from 250 to 320 K. The ΔF^{host} values for release curves are shown in Figure S13 and are compared with the ΔF^{host} values obtained from the desorption branches of the pure CO_2 experimental isotherms (Model 1).

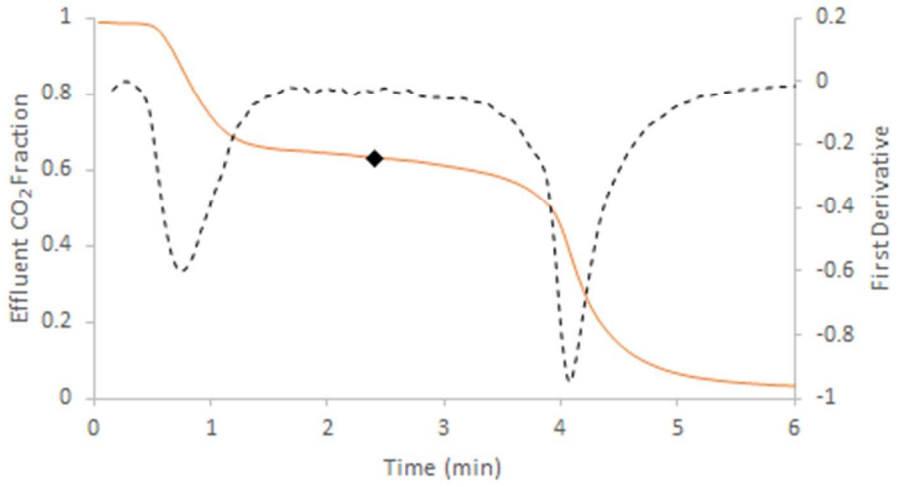

Figure S12. Determination of the step level (black diamond) using the first derivative (black dashed line) of an experimentally measured CO_2 release curve (orange solid line). In the breakthrough experiment shown, pure CH_4 is displacing pure CO_2 ($CH_4 \rightarrow CO_2$) at 302 K.

For the He→CO_2 release curves (r^2 = 0.848):

$$\Delta F^{host}(T)\left[\frac{J}{mol}\right] = 325.58 * T - 76983 \quad \text{(S3)}$$

For the N_2→CO_2 release curves (r^2 = 0.963):

$$\Delta F^{host}(T)\left[\frac{J}{mol}\right] = 261.61 * T - 54058 \quad \text{(S4)}$$

For the CH_4→CO_2 release curves (r^2 = 0.072):

$$\Delta F^{host}(T)\left[\frac{J}{mol}\right] = 12.139 * T + 27143 \quad \text{(S5)}$$

For the CO_2/Mix→He breakthrough curves (r^2 = 0.549):

$$\Delta F^{host}(T)\left[\frac{J}{mol}\right] = 409.79 * T - 86409 \quad \text{(S6)}$$

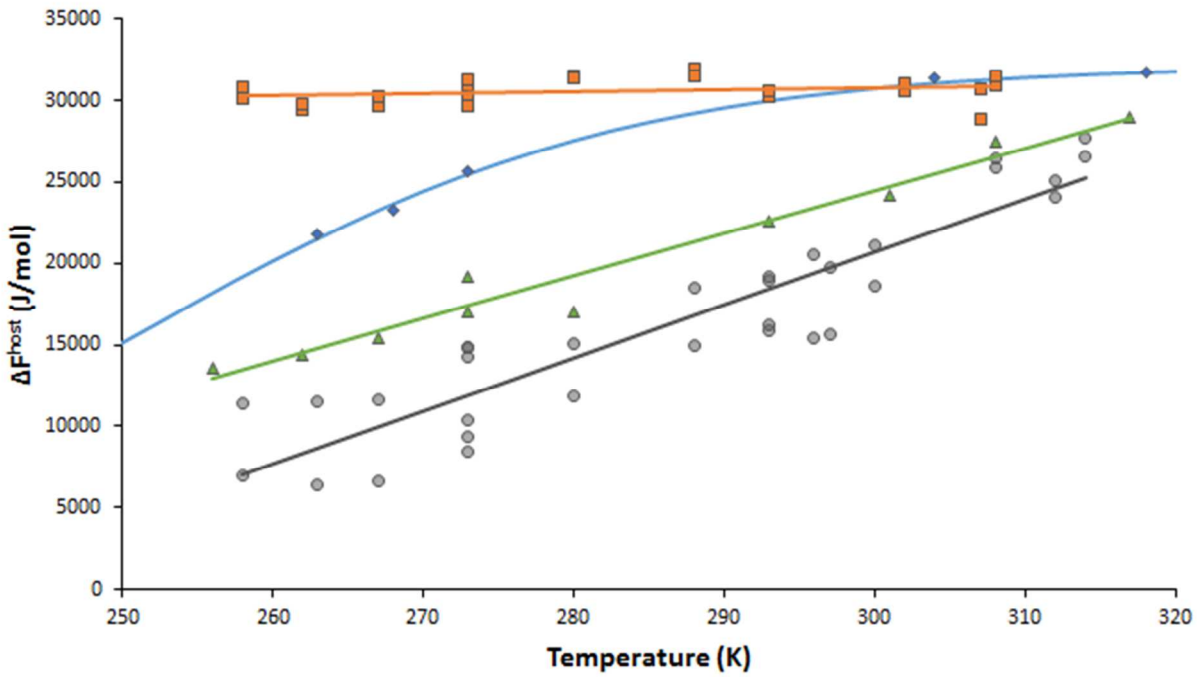

Figure S13. Comparison of ΔF^{host} values obtained using Model 1 (blue diamonds) with those obtained using Model 3. CO_2 release curves are shown where the flush gas is helium (He→CO_2) (grey circles), nitrogen (N_2→CO_2) (green triangles), and methane (CH_4→CO_2) (orange squares).

Section S4. Sample MATLAB code for OFAST. The following code was used to estimate mixture co-adsorption for a range of temperatures (250 to 350 K), mixture compositions (5 to 95% CO_2), and pressures (5 to 500 kPa) on the expanded ELM-11 structure using the OFAST method with IAST. The code also estimates the gate pressure for a particular temperature and mixture composition.

```
%Define other factors
R = 8.314462;

%initial Dummy Matrix
P_out = zeros(399,11);
Pgate_out = zeros(399,3);
CoefOpen = zeros(399,4);
P_all = zeros(100,1);
Ntot_o = zeros(100,1);

% Set up fittype and options.
ft = fittype( 'k*x/(1+k*x/n)', 'independent', 'x', 'dependent', 'y' );
opts = fitoptions( 'Method', 'NonlinearLeastSquares' );
opts.Display = 'Off';
opts.Lower = [0 0];
opts.Robust = 'LAR';
opts.StartPoint = [1 8];

L = 32173.95434;
A = 8989582.641;
a = 0.063566682;

for t = 1:1:21; %runnning through variable Tempts
    T = 245+5*t
    deltaFhost = L/(1+A*exp(-1*a*T));%Fhost fit to temp (logistic Fit)

    %Open Structure
    %langmuir parameters for CO2 (Fit by Temp)
    Nb = 15.741-0.0238*T;
    Kb = exp(2110.9*1/T-7.9214);
    %then langmuir parameters for He(Fit by temp)
    Nc = 0.0552*T - 2.3106;
    Kc = exp(473.18*1/T - 10.831);

    %Closed Structure: Not Used Here

    for j = 1:1:19;
        %defining the mol fraction y of the mix
        yb = j*0.05; %i.e. mix is (j*0.05)% CO2
        yc = 1-yb;
        %timer = j
```

```
        %develop a For loop to calculate all Pbs and  from 5 to 500 kPa
        for n = 1:1:100
            %set the pressure in kpa
            P = n*5;
            %Now I want to solve for Pb* (denoted Pb)
            syms x; %denotes x as a dummy variable
            Pb = vpasolve(P*yc*x/(x-P*yb) == Nc/Kc*((1+Kb*x/Nb)^(Nb/Nc)-
1),x,P*yb*1.001);

            %calculate the rest
            %Open
            xb = P*yb/Pb; %fraction CO2 adsorbed
            xc = 1-xb; %fraction He adsorbed

            Pc = (P - Pb*xb)/(1-xb); %fictitious pressure Pc*
            Nb_fic = Kb*Pb/(1+Kb*Pb/Nb); %fictitious amount of CO2, CO2 sees
            Nc_fic = Kc*Pc/(1+Kc*Pc/Nc); %ficticious amount of He, He sees
            Ntot = 1/(xb/Nb_fic + xc/Nc_fic); %calculation of N total
            alpha = (xb/xc)/(yb/yc); %calculation of selectivity

            %output to matrix
            P_all(n,1)= P;
            Ntot_o(n,1)= Ntot;

            if P==100;
                P_out(j+19*(t-1),1)= P;
                P_out(j+19*(t-1),2)= T;
                P_out(j+19*(t-1),3)= yb;
                P_out(j+19*(t-1),4)= Pb;
                P_out(j+19*(t-1),5)= Pc;
                P_out(j+19*(t-1),6)= xb;
                P_out(j+19*(t-1),7)= xc;
                P_out(j+19*(t-1),8)= Nb_fic;
                P_out(j+19*(t-1),9)= Nc_fic;
                P_out(j+19*(t-1),10)= Ntot;
                P_out(j+19*(t-1),11)= alpha;
            end
        end

        % Fit model to data.
        [fitresult, gof] = fit( P_all, Ntot_o, ft, opts );
        CoefOpen(j+19*(t-1),1) = yb;
        CoefOpen(j+19*(t-1),2) = fitresult.k;
        CoefOpen(j+19*(t-1),3) = fitresult.n;
        CoefOpen(j+19*(t-1),4) = gof.rsquare;

        K2 = CoefOpen(j+19*(t-1),2);
        N2 = CoefOpen(j+19*(t-1),3);

        Pgate = vpasolve(0==deltaFhost - R*T*(N2*log(1+K2*x/N2)),x,60);
        Pgate_out(j+19*(t-1),1) = T;
        Pgate_out(j+19*(t-1),2) = yb;
        Pgate_out(j+19*(t-1),3) = Pgate;
    end
```

```
end

for i = 1:1:399
    if P_out(i,1)<Pgate_out(i,3)
        P_out(i,4)= 0;
        P_out(i,5)= 0;
        P_out(i,6)= 0;
        P_out(i,7)= 0;
        P_out(i,8)= 0;
        P_out(i,9)= 0;
        P_out(i,10)= 0;
        P_out(i,11)= 0;
    end
end
```

Section S5. GCMC Simulation Details. Isotherms for He, N_2, and CH_4 on the expanded ELM-11 structure were generated using grand canonical Monte Carlo (GCMC) simulation performed in the MCCCS Towhee package[3]. The simulation cell used triclinic periodic boundary conditions with constant temperature, volume, and adsorbent-adsorbate chemical potentials. Trial moves for adsorbate molecules included translation, insertion, and deletion. Simulations for linear N_2 also included molecular rotation. Each non-orthogonal simulation cell contained ten 4x8 layers of ELM-11, corresponding to a total of 320 Cu atoms. Figure S14 shows an overhead view of one of the 4x8 layers of the expanded ELM-11 structure used in the simulation. Figure S15 shows a corresponding side view. Simulations were run for 10 million sampled moves, with the first 2.5 million moves removed from the analysis as a pre-equilibration phase.

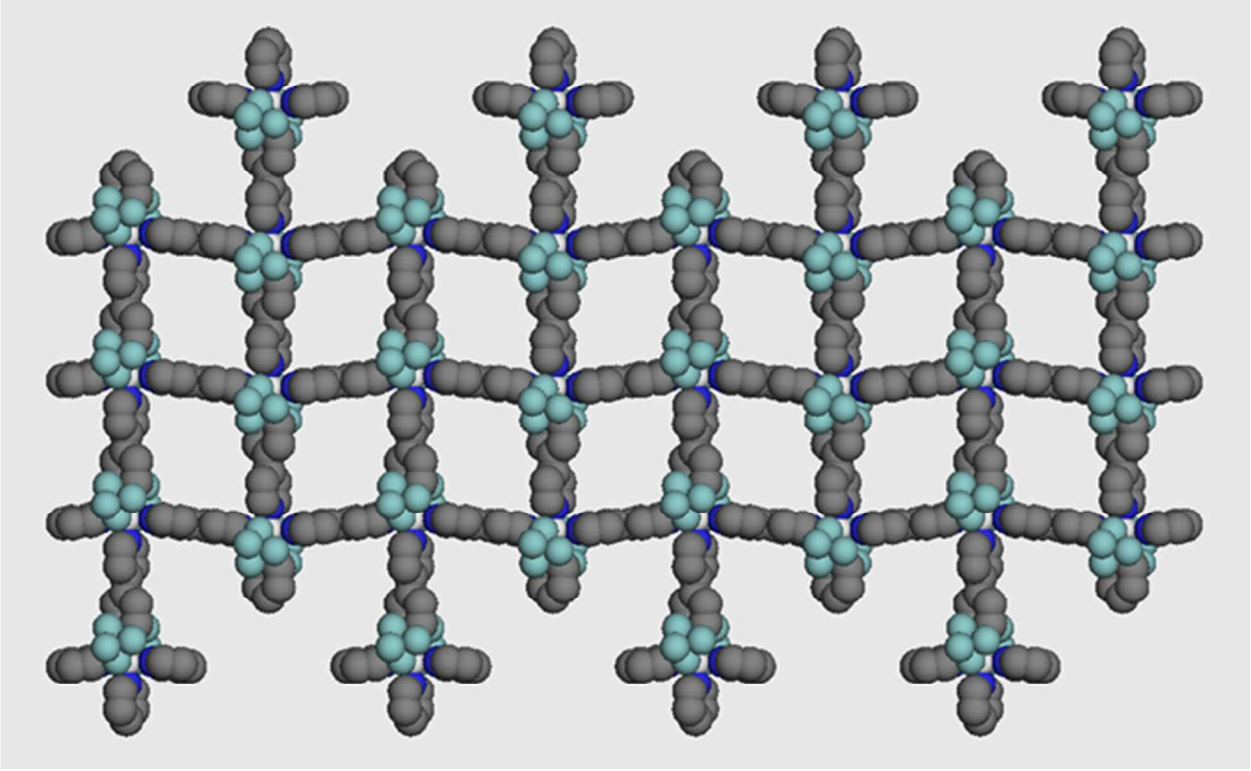

Figure S14. Overhead view of one 4x8 layer of ELM-11 used in GCMC simulation cell. Bipyridine linkers are shown in black (carbon) and navy blue (nitrogen), Copper is shown in white, and tetrafluoroborate is shown in light blue.

The three-site TraPPE-EH force field[4] was used for N_2 and the single site TraPPE-UA force field[5,6] was used for He and CH_4. The DREIDING force field[7] was used for the ELM-11 structure. The parameters for Fe^{2+} were used for Cu^{2+} in the ELM-11 model, because the DREIDING force field employed in towhee does not include an entry for Cu^{2+} and that information is not available in molecular simulation force fields. DREIDING does, however, include parameters for Fe^{2+} and Zn^{2+}, which bracket Cu on the periodic table. DREIDING also uses the same Lennard-Jones parameters for both Fe^{2+} and Zn^{2+}. Note that the Cu atoms in ELM-11 are encapsulated between the bpy ligands and BF_4 counter ions and are not directly accessible to adsorbing molecules (i.e., they are not open metal sites).

Charge assignments for atoms in the ELM-11 structure were determined from density functional theory calculations performed using the Gaussian 09 software package[11]. After geometric optimization of a unit cluster of ELM-11, atomic partial charges were derived from

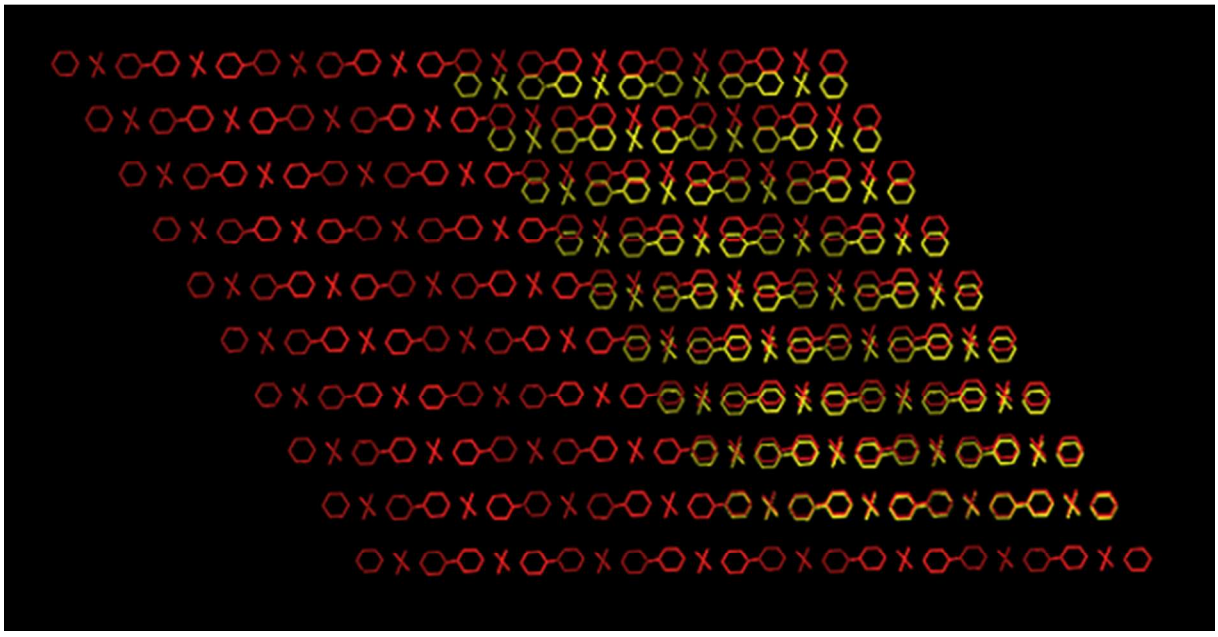

Figure S15. Shown in red is a side view of ten 4x8 layers of the ELM-11 5% expanded structure used in the simulation cell. Shown in yellow is a ten 4x4 layers of the unexpanded structure for comparison. Tetrafluoroborate ions have been removed for clarity.

calculated Mulliken charges. To remove ambiguity about the simulation system, a sample MCCCS Towhee input file has been provided in section S6.

Use of the DREIDING force field for the simulation of adsorption in ELM-11 has not previously been reported. However, in general, Lennard-Jones potentials with DREIDING or UFF parameters for framework atoms and TraPPE parameters for CH_4 result in good models for understanding CH_4 adsorption in MOFs.[8] Tanaka et al.[10] successfully used the UFF force field to model CO_2 adsorption in ELM-11 for their investigation of gate opening. Previous work has shown that similar results for CH_4 isotherms on IRMOF-1 and IRMOF-6 at 298 K can be obtained using the DREIDING and UFF force fields, suggesting that, at least for some MOFs, simulation results are not very sensitive to the choice of the framework parameter set.[8]

Given that the GCMC simulated CH_4 adsorption isotherms agreed reasonably well with the experimental CH_4 isotherms on ELM-11 reported by Kanoh et al.[9], the simulation model and produced isotherms were deemed sufficient for an investigation into the use of IAST within OFAST to predict the breakthrough curve features of flexible framework adsorbents. It should be noted that the 5% expanded ELM-11 structure referenced in the main manuscript may not be the most relevant structure for simulating N_2 or He isotherms, which have smaller kinetic diameters than CH_4, and N_2 adsorbed amounts were significantly higher on the 5% expanded structure as compared with original structure. However, overestimation of N_2 and He loadings on ELM-11 due to an estimated framework interlayer distance that is too large would not explain the results obtained from OFAST model 2.

Section S6. Sample Towhee Input File. The following sample towhee code was used to determine quantity of N_2 adsorbed onto the expanded ELM-11 structure at 273 K and 25 kPa.

```
inputformat
'Towhee'
randomseed
1302002
random_luxlevel
3
random_allow_restart
T
ensemble
'uvt'
temperature
273.0
nmolty
2
nmolectyp
320 900
chempot
# 273k 25kpa n2
0.0         -4574.74111
numboxes
   1
stepstyle
'moves'
nstep
   10000000
printfreq
   500000
blocksize
   500000
moviefreq
   1000000
backupfreq
   500000
restartfreq
   0
runoutput
'full'
pdb_output_freq
   500000
loutdft
   F
loutlammps
   F
loutdlpoly
   F
louthist
   T
hist_label
   1
hist_suffix
   a
```

hist_nequil
0
histcalcfreq
100000
histdumpfreq
100000
pressurefreq
300000
trmaxdispfreq
100000
volmaxdispfreq
100000
chempotperstep
0 0 0
potentialstyle
'internal'
ffnumber
5
ff_filename
/home/software/rhel5/towhee/6.2.7/ForceFields/towhee_ff_DREIDING
/home/software/rhel5/towhee/6.2.7/ForceFields/towhee_ff_TraPPE-EH
/home/software/rhel5/towhee/6.2.7/ForceFields/towhee_ff_TraPPE-UA
classical_potential
'Lennard-Jones'
classical_mixrule
'Lorentz-Berthelot'
lshift
F
ltailc
F
rmin
1.0
rcut
14.000000000000
rcutin
5.0000000000000
electrostatic_form
'coulomb'
coulombstyle
'ewald_fixed_kmax'
kalp
5.6
kmax
5
dielect
1.0
nfield
0
solvation_style
'none'
linit
T
initboxtype
'dimensions'
initstyle
'coords' 'coords' 'coords'

initlattice
'none' 'none' 'none'
initmol
320 0
inix iniy iniz
8 4 10
hmatrix
#ELM-11 105 expand 2x box
88.42020264 0.00000000 0.00000000
0.00000054 44.28800000 0.00000000
36.81288905 55.36000048 60.66189212
pmuvtcbswap
0.4
pmuvtcbmt
0.0 1.0
pmtracm
0.7
pmtcmt
0.0 1.0
rmtrac
0.5000
tatrac
0.5000
pmrotate
1.0
pmromt
0.0 1.0
rmrot
0.0500
tarot
0.5000
cbmc_style
'coupled-decoupled'
coupled_decoupled_form
'Martin and Siepmann JPCB 1999'
cbmc_setting_style
'default ideal'
#Cu_MOF-2a 2x4x10 DREIDING implicit H no bonds
input_style
'basic connectivity map'
nunit
35
nmaxcbmc
35
lpdbnames
F
forcefield
'DREIDING'
charge_assignment
'manual'
unit ntype qqatom
1 Fe_+2 0.52800
vibration
0
improper torsion
0

unit ntype qqatom
2 B_3 0.84300
vibration
0
improper torsion
0
unit ntype qqatom
3 B_3 0.84300
vibration
0
improper torsion
0
unit ntype qqatom
4 F_ -0.40900
vibration
0
improper torsion
0
unit ntype qqatom
5 F_ -0.36000
vibration
0
improper torsion
0
unit ntype qqatom
6 F_ -0.36000
vibration
0
improper torsion
0
unit ntype qqatom
7 F_ -0.36000
vibration
0
improper torsion
0
unit ntype qqatom
8 F_ -0.40900
vibration
0
improper torsion
0
unit ntype qqatom
9 F_ -0.36000
vibration
0
improper torsion
0
unit ntype qqatom
10 F_ -0.36000
vibration
0
improper torsion
0
unit ntype qqatom
11 F_ -0.36000

vibration
0
improper torsion
0
unit ntype qqatom
12 C_R 0.07400
vibration
0
improper torsion
0
unit ntype qqatom
13 C_R1 0.00100
vibration
0
improper torsion
0
unit ntype qqatom
14 C_R1 0.25900
vibration
0
improper torsion
0
unit ntype qqatom
15 C_R 0.07400
vibration
0
improper torsion
0
unit ntype qqatom
16 C_R1 0.00100
vibration
0
improper torsion
0
unit ntype qqatom
17 C_R1 0.25900
vibration
0
improper torsion
0
unit ntype qqatom
18 C_R1 0.00100
vibration
0
improper torsion
0
unit ntype qqatom
19 C_R1 0.25900
vibration
0
improper torsion
0
unit ntype qqatom
20 C_R 0.07400
vibration
0

improper torsion
0
unit ntype qqatom
21 C_R1 0.25900
vibration
0
improper torsion
0
unit ntype qqatom
22 C_R1 0.00100
vibration
0
improper torsion
0
unit ntype qqatom
23 C_R1 0.00100
vibration
0
improper torsion
0
unit ntype qqatom
24 C_R1 0.25900
vibration
0
improper torsion
0
unit ntype qqatom
25 C_R1 0.00100
vibration
0
improper torsion
0
unit ntype qqatom
26 C_R1 0.25900
vibration
0
improper torsion
0
unit ntype qqatom
27 C_R1 0.00100
vibration
0
improper torsion
0
unit ntype qqatom
28 C_R1 0.25900
vibration
0
improper torsion
0
unit ntype qqatom
29 C_R   0.07400
vibration
0
improper torsion
0

```
unit ntype qqatom
30 C_R1  0.25900
vibration
0
improper torsion
0
unit ntype qqatom
31 C_R1  0.00100
vibration
0
improper torsion
0
unit ntype qqatom
32 N_R   -0.40300
vibration
0
improper torsion
0
unit ntype qqatom
33 N_R   -0.40300
vibration
0
improper torsion
0
unit ntype qqatom
34 N_R   -0.40300
vibration
0
improper torsion
0
unit ntype qqatom
35 N_R   -0.40300
vibration
0
improper torsion
0
# TraPPE-EH N2
input_style
'basic connectivity map'
nunit
   3
nmaxcbmc
   3
lpdbnames
   F
forcefield
'TraPPE-EH'
charge_assignment
'manual'
unit ntype qqatom
1    'COM_n2'    0.964
vibration
2
2 3
improper torsion
0
```

unit ntype qqatom
2 'N_n2' -0.482
vibration
1
1
improper torsion
0
unit ntype qqatom
3 'N_n2' -0.482
vibration
1
1
improper torsion
0

REFERENCES

(1) Coudert, F.-X. The Osmotic Framework Adsorbed Solution Theory: Predicting Mixture Coadsorption in Flexible Nanoporous Materials. *Phys. Chem. Chem. Phys.* **2010**, *12* (36), 10904.

(2) MATLAB and Statistics Toolbox. *Version 8.5.0 (R2015a)*; The MathWorks, Inc., Natick, Massachusetts, United States, 2015.

(3) Martin, M. G. MCCCS Towhee: A Tool for Monte Carlo Molecular Simulation. *Mol. Simul.* **2013**, *39* (14–15), 1212–1222.

(4) Potoff, J. J.; Siepmann, J. I. Vapor–liquid Equilibria of Mixtures Containing Alkanes, Carbon Dioxide, and Nitrogen. *AIChE J.* **2001**, *47* (7), 1676–1682.

(5) Martin, M. G.; Siepmann, J. I. Calculating Gibbs Free Energies of Transfer from Gibbs Ensemble Monte Carlo Simulations. *Theor. Chem. Accounts Theory, Comput. Model. (Theoretica Chim. Acta)* **1998**, *99* (5), 347–350.

(6) Martin, M. G.; Siepmann, J. I. Transferable Potentials for Phase Equilibria. 1. United-Atom Description of N-Alkanes. *J. Phys. Chem. B* **1998**, *102*, 2569–2577.

(7) Mayo, S. L.; Olafson, B. D.; Goddard, W. A. DREIDING: A Generic Force Field for Molecular Simulations. *J. Phys. Chem.* **1990**, *94* (26), 8897–8909.

(8) Getman, R. B.; Bae, Y.; Wilmer, C. E.; Snurr, R. Q. Review and Analysis of Molecular Simulations of Methane, Hydrogen, and Acetylene Storage in Metal–Organic Frameworks. *Chem. Rev.* **2012**, *112* (2), 703–723.

(9) Kanoh, H.; Kondo, A.; Noguchi, H.; Kajiro, H.; Tohdoh, A.; Hattori, Y.; Xu, W.-C.; Inoue, M.; Sugiura, T.; Morita, K.; et al. Elastic Layer-Structured Metal Organic Frameworks (ELMs). *J. Colloid Interface Sci.* **2009**, *334* (1), 1–7.

(10) Tanaka, H.; Hiraide, S.; Kondo, A.; Miyahara, M. T. Modeling and Visualization of CO2 Adsorption on Elastic Layer-Structured Metal–Organic Framework-11: Toward a Better Understanding of Gate Adsorption Behavior. *J. Phys. Chem. C* **2015**, *119* (21), 11533–11543.

(11) Gaussian 09. *Frisch, G. W. Trucks, H. B. Schlegel, G. E. Scuseria, M. A. Robb, J. R. Cheeseman, G. Scalmani, V. Barone, B. Mennucci, G. A. Petersson, H. Nakatsuji, M. Caricato, X. Li, H. P. Hratchian, A. F. Izmaylov, J. Bloino, G. Zheng, J. L. Sonnenberg, M. Hada, M.* ; Gaussian, Inc., Wallingford CT, 2010.